

Mu-Mesonic Atoms and the Electromagnetic Radius of the Nucleus

L. N. COOPER AND E. M. HENLEY*

Department of Physics, Columbia University, New York, New York

(Received July 22, 1953)

An attempt is made to interpret recent experiments on the x-ray spectrum of μ^- -mesonic atoms. In particular, an analysis is made of the $2p-1s$ transition energies, which are sensitive to the nuclear charge distribution. Agreement with experiment is obtained for a uniform sphere of nuclear charge of radius $R \approx 1.2 \times 10^{-13} A^{1/3}$ cm. Various effects such as nuclear polarization, electric quadrupole moment, screening by atomic electrons, and a meson-nucleon interaction of the order indicated by the charge exchange capture reaction are considered and do not alter this radius appreciably. However, an anomalous meson-nucleus interaction, though doubtful, could alter the estimated radius. It is shown that the small nuclear radius is not in disagreement with that determined by other electromagnetic measurements, including mirror nuclei experiments.

INTRODUCTION

THE discovery by Conversi, Pancini, and Piccioni¹ of the smallness of the μ^- -nuclear interaction and the resulting realization that the μ meson was not the Yukawa particle, although originally a great disappointment to theoretical physicists, has led to an interesting and useful tool with which the nucleus can be probed.

It was soon realized^{2,3} that a relativistic μ meson can be slowed down in condensed matter, captured in bound states about a nucleus, and can make transitions to the lowest bound states in a time short compared to that for meson decay or nuclear capture. Thus there seemed to be a strong possibility that μ -mesonic atoms could be produced. Such atoms are of great interest because an investigation of their spectra might yield information about the nuclear proton distribution. Furthermore, if spectra of sufficient accuracy could be obtained, the spin, magnetic moment, and mass of the μ meson could be determined independently of other measurements. This was suggested by Wheeler,⁴ and a study of μ^- -mesonic atomic spectra has been carried out by Fitch and Rainwater.⁵

When first captured by an atom the μ^- meson interacts with the atomic electrons and with the nucleus, cascading down to the lower orbits through radiative and electronic processes. The highest angular momentum states are preferred for statistical reasons, and there is a large probability that the meson will fall to a $2p$ state. This is enhanced by the absence of a metastable $2s$ level. In the mesonic atom the $2s$ level is above the $2p$ level because of the extension of the nucleus. Wheeler⁴ has shown that for Z larger than 15 the probability of radiative transitions among the lowest orbits is overwhelmingly larger than that of electronic (such as Auger) transitions. Thus a $2p-1s$ radiative transition is expected. A transition to the $1s$ state is of

particular interest because the $1s$ level is most sensitive to the nuclear charge distribution. (The higher levels progressively become more hydrogen-like.) The energy and intensity of the x-rays emitted in the $2p-1s$ transition make them easiest to observe, and it is these x-rays that Fitch and Rainwater have studied.

The use of the μ^- meson as a nuclear probe is possible because the mesonic orbits are much closer to the nucleus than the corresponding electron orbits. This is due to the meson-to-electron-mass ratio, which is about 210. For heavy elements, the average radius of the meson ground state may lie inside the nucleus. In the case of lead for example, the probability of finding the $1s$ -state meson inside the nucleus is approximately one half. For the heavy elements therefore, the lowest meson energy levels and transition energies are very sensitive to the nuclear charge distribution.

The effect of the atomic electrons on the lowest meson energy levels can be calculated by considering the screening effect of the electrons as decreasing the effective nuclear charge. The p -level shift for a heavy element such as lead is about 0.005 Mev or 0.1 percent of the p -state energy, while for a lighter element such as copper the corresponding shift is about 0.002 Mev or 0.3 percent of the orbit energy. We can therefore neglect the interaction of the meson with the atomic electrons in calculating the expected energy of the radiation emitted in the lowest-level transitions of the meson, and can treat the meson and nucleus as an isolated system.

When the experiment is carried out for an element with several isotopes, the chief effect to be expected with the present resolution is a broadening of the observed spectrum lines.

There are two distinct interactions of the meson with a nucleus. One is the electromagnetic interaction, which, as Wheeler has shown,⁴ is predominant, while the other—a specific nuclear interaction such as that leading to the charge-exchange-capture reaction—is much smaller.

The electromagnetic interaction itself can be divided into static and dynamic interactions. These latter give rise to such refinements in the spectrum as hyperfine

* Frank B. Jewett Fellow.

¹ Conversi, Pancini, and Piccioni, *Phys. Rev.* **71**, 209 (1947).

² Fermi, Teller, and Weisskopf, *Phys. Rev.* **71**, 314 (1947).

³ E. Fermi and E. Teller, *Phys. Rev.* **72**, 399 (1947).

⁴ J. A. Wheeler, *Revs. Modern Phys.* **21**, 133 (1949).

⁵ V. L. Fitch and J. Rainwater, *Phys. Rev.* (preceding paper) *Phys. Rev.* **92**, 789 (1953).

structure, which are very small. For aluminum, with spin 5/2, the splitting effect due to the interaction with the nuclear magnetic moment is about 10 ev.⁴ For lead, Pb²⁰⁷, the corresponding number is about 3 kev.

In Sec. I it is shown that the energy levels of a μ^- -mesonic atom can be obtained by considering the meson to move in the electric potential produced by a uniformly charged spherical nucleus. In addition, for light nuclei, the shift of the $2p-1s$ transition energy resulting from the extent of the nucleus is shown to depend only on the second moment of the charge distribution.

In Sec. II we consider the dependence of these energy levels on (1) meson properties, (2) the assumed nuclear ground-state charge distribution, (3) nuclear polarization effects, and (4) anomalous meson nuclear interactions.

In Sec. III the results of the μ^- -meson experiment are compared with other measurements of the nuclear radius. Electromagnetic radii, as measured by high-energy electron and proton scattering and by isotope shifts, are consistent with the present experiment. We show that mirror nuclei radius measurements cannot be made consistent with the above by charge-distribution variations alone. However, inclusion of the Coulomb exchange energy and angular momentum effects in the calculation of the energy change in mirror nuclei transitions removes the discrepancy.

I. ENERGY LEVELS OF THE MESONIC ATOM

The entire meson-nucleus interaction can be divided into two parts, one of which is electromagnetic in origin, while the other is a specific nuclear interaction. Because of the smallness of the nuclear term, it is possible to calculate the energy levels of the meson-nucleus system by considering only the electromagnetic interaction and treating the nuclear interaction as a perturbation.

The Schrödinger equation for the meson-nucleus system is then

$$H\Psi = (H^N + H^\mu + H^e)\Psi = W\Psi, \quad (1)$$

where H^N is the total nuclear Hamiltonian, H^μ is the free meson Hamiltonian, and H^e is the electromagnetic interaction of the meson and nucleus.

In this treatment the μ^- meson is taken to have a spin⁶ of $\frac{1}{2}$ and to satisfy the Dirac equation; thus H^μ is

$$H^\mu = \alpha \cdot \mathbf{p} + \beta\mu.$$

($\hbar=c=1$ is used throughout.) α and β are the usual Dirac matrices, and μ is the meson mass.

In the electromagnetic interaction term the nucleus is not treated as a point charge, since for heavy elements the meson may spend a considerable portion of its time inside nuclear matter. For a nucleus with Z

protons H^e is

$$H^e = \sum_{i=1}^Z \left(-\frac{e^2}{|\mathbf{r} - \mathbf{R}_i|} \right), \quad (2)$$

where \mathbf{R}_i is the position vector of the i th proton and \mathbf{r} is the position vector of the μ^- meson.

The wave function for the meson-nucleus system can be separated if we assume that the nucleus is unaffected by the presence of the meson. Such an assumption is a legitimate first approximation because the meson-nucleus interaction is small compared to the forces which bind the nucleus. With this assumption, Ψ becomes

$$\Psi(\mathbf{R}_1 \cdots \mathbf{R}_i \cdots \mathbf{R}_Z, \mathbf{r}) = \psi(\mathbf{R}_1 \cdots \mathbf{R}_i \cdots \mathbf{R}_Z) \Phi(\mathbf{r}),$$

and H^e can be replaced by

$$\langle \psi_0 | H^e | \psi_0 \rangle \equiv V, \quad (3)$$

where $\psi(\mathbf{R}_1 \cdots \mathbf{R}_Z)$ is the nuclear wave function (ψ_0 is the ground state) and $\phi(\mathbf{r})$ is the meson wave function. In this case Eq. (1) becomes

$$H^N \psi = E \psi, \quad (4a)$$

and

$$(H^\mu + V) \Phi = \epsilon \Phi. \quad (4b)$$

W is thus $W = E + \epsilon$, where E is the nuclear and ϵ the mesonic energy.

If the nuclear ground-state charge distribution is taken to be uniform

$$\begin{aligned} \rho(\mathbf{R}_i) &= \text{constant} & R_i < R \\ \rho(\mathbf{R}_i) &= 0 & R_i > R, \end{aligned} \quad (5)$$

then the potential V becomes

$$\begin{aligned} V &= -\frac{Ze^2}{R} \left(\frac{3}{2} - \frac{1}{2} \frac{r^2}{R^2} \right) & r \leq R \\ &= -\frac{Ze^2}{r} & r \geq R, \end{aligned} \quad (6)$$

where R is the nuclear radius. Equation (4b) is then the Dirac equation for a charged particle in the potential of a uniform sphere of charge Ze . This can be expanded into large and small components because the meson nucleus system is not very relativistic. From Eq. (6), the minimum potential, $-3Ze^2/2R$, is seen to occur at the center of the nucleus and to decrease with Z . Even for a heavy element such as lead $|V|_{\text{max}}$ is only approximately 25 Mev, which is much smaller than the meson rest mass of 107 Mev. The equation for the large components may be written as

$$\left[H_S - \frac{(\epsilon - V)^2}{2\mu} + \frac{1}{8\mu^2} \nabla^2 + \frac{1}{2\mu^2} \frac{1}{r} \frac{dV}{dr} \mathbf{L} \cdot \mathbf{S} \right] \phi_L = \epsilon \phi_L, \quad (7)$$

⁶ J. Tiomno and J. A. Wheeler, *Revs. Modern Phys.* **21**, 144 (1949).

where H_S is the Schrödinger Hamiltonian, $H_S = -\nabla^2/2\mu + V$, and the last term is the spin-orbit interaction. We have solved this equation, treating the relativistic terms as perturbations on the Schrödinger solution. This can be shown to give energies that are accurate to better than 1 percent. The eigenvalues of the Schrödinger equation are obtained by matching the logarithmic derivatives of the internal and external wave functions at the edge of the nucleus. The internal wave function is⁷

$$\phi_{ei}(\text{internal}) \sim \exp(-\beta^2 \rho^2/2) (\beta \rho)^l \lim_{b \rightarrow \infty} F(\gamma, b, l+3/2; \rho^2/b). \quad (8a)$$

For $l=0$, this can be written simply as

$$\phi_{e0}(\text{internal}) \sim \exp(-\beta^2 \rho^2/2) \mathcal{H}_0(\beta \rho). \quad (8b)$$

Here $\rho = (8\mu\epsilon)^{1/2} r$, $\beta^4 = Ze^2/(64\mu\epsilon^2 R^3)$, $\gamma = \Gamma - (l+1)$, $\Gamma = (3Ze^2/8\epsilon R - \frac{1}{2})/2\beta^2 - \frac{1}{2}$, l is the angular momentum of the state of energy ϵ , F is the hypergeometric series,⁷ and \mathcal{H} is that solution to the Hermite differential equation⁷ which is zero at the origin. The external wave function is

$$\phi_{ei}(\text{external}) \sim \rho^{-1} W_{k, [\Gamma(l+1) + \frac{1}{2}]}(\rho), \quad (9)$$

where $k = Ze^2(\mu/2\epsilon)^{1/2}$ and W is the confluent hypergeometric function.⁸

The corrections to the nonrelativistic energy levels due to the Dirac terms in Eq. (7) are of the order of 2 percent for lead and copper. The essential nonrelativistic motion of the meson allows us to treat corrections such as those arising from polarization as perturbations on the nonrelativistic solutions.

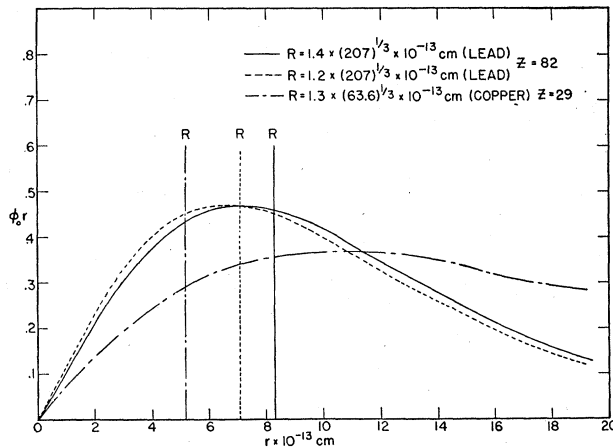


FIG. 1. Normalized, nonrelativistic 1s-state meson wave functions for copper and lead. The nuclear charge distribution is taken to be uniform and of radius $R = r_0 A^{1/3}$.

⁷ E. U. Condon and P. M. Morse, *Quantum Mechanics* (McGraw-Hill Book Company, Inc., New York, 1929), p. 79; H. Margenau and G. M. Murphy, *The Mathematics of Chemistry and Physics* (D. Van Nostrand and Company, New York, 1943), pp. 72, 76.

⁸ E. T. Whittaker and G. N. Watson, *Modern Analysis* (MacMillan Company, New York, 1944), Chap. 16, especially p. 343.

TABLE I. Experimental and calculated $2p-1s$ transition energies. The meson mass is taken as $210m_e$.

Element	Z	Experimental $2p_{3/2}-1s_{1/2}$ energy Mev	Calculated r_0 (to fit experiment) ($\times 10^{-13}$ cm)	Calculated $1s_{1/2}$ energy Mev	Calculated $2p_{3/2}-1s_{1/2}$ energy Mev	Calculated $2p_{1/2}-1s_{1/2}$ energy Mev
$R = 1.3 \times 10^{-13} \times A^{1/3}$ cm						
Aluminum	13	0.35				
Silicon	14	0.41				
Titanium	22	0.955	1.17	1.282	0.935	0.933
Copper	29	1.55	1.21	2.12	1.52	1.51
Zinc	30	1.60				
Antimony	51	3.50	1.22	5.22	3.41	3.37
Mercury	80	5.80				
Lead	82	6.02	1.17	10.11	5.48	5.30
Bismuth	83	6.02				

Fitch and Rainwater have solved the Dirac Eq. (4b) without expansion into large and small components and by other methods described in the preceding paper. For the elements we have treated, our calculated energy levels agree with theirs to within 1 percent. Their experimental and calculated results are repeated in Table I below. Our nonrelativistic wave functions for the $1s$ level of lead ($r_0 = 1.4$ and 1.2×10^{-13} cm) and copper ($r_0 = 1.3 \times 10^{-13}$ cm) are plotted in Fig. 1.

It is seen from Table I that for a meson mass of $210m_e$ and a nuclear radius larger or equal to $1.3 \times 10^{-13} A^{1/3}$ cm (as expected from other data⁹), the calculated $2p_{3/2}-1s_{1/2}$ transition energies are consistently smaller than those observed. A radius $R \approx 1.2 \times 10^{-13} A^{1/3}$ cm, on the other hand, is consistent with the experimental data for all elements.

For light nuclei it is possible to treat the energy shifts due to both nuclear extension and relativistic effects as perturbations on the Schrödinger equation for a point charge. The correction due to nuclear extension $\Delta\epsilon_R$ is negligible for all but the $1s$ state. The corrections due to both effects may be computed as a power series expansion in $Z\alpha$ and $Z\alpha\mu R$, where α is the fine structure constant. For an arbitrary charge distribution the leading term in the expansion of $\Delta\epsilon_R$ is

$$\begin{aligned} \Delta\epsilon_R &= \langle \phi_0 | V - V_p | \phi_0 \rangle \\ &= -\frac{1}{\pi} (Z\alpha\mu)^3 \int (V - V_p) dx + \dots \\ &= -\frac{1}{6\pi} (Z\alpha\mu)^3 \int \rho r^2 dx + \dots, \end{aligned} \quad (10)$$

where the latter equality holds if

$$\lim_{r \rightarrow \infty} r^3 (V - V_p) = 0.$$

In Eq. (10) ϕ_0 is the nonrelativistic hydrogen-like wave function for the mesonic $1s$ level; V is defined by Eq.

⁹ J. M. Blatt and V. E. Weisskopf, *Theoretical Nuclear Physics* (John Wiley and Sons, Inc., New York, 1952), pp. 14-15.

(3), V_p is the interaction energy of a point nucleus with the μ meson, $V_p = -Ze^2/r$, and ρ is the charge density corresponding to V , $\rho = -\nabla^2 V$. For light nuclei, therefore, it is essentially only the second moment of the charge distribution which is determined by the x-ray transitions observed by Fitch and Rainwater. It is of interest to note that the integral in Eq. (10) determines the change in the cross section for the scattering by nuclei of high-energy electrons (less than ~ 40 Mev) when the nucleus is an extended source rather than a point charge, as was shown by Feshbach.¹⁰

For a uniform charge distribution Eq. (10) gives

$$\Delta\epsilon_R = -\frac{2}{5}\mu(Z\alpha)^2(Z\alpha\mu R)^2. \quad (11)$$

The dependence of the leading term in $\Delta\epsilon_R$ on Z and R , as given by Eq. (11) is quite general. This can be seen from Eq. (10), since $\int \rho r^2 d\mathbf{r}$ is proportional to ZR^2 . Hence $\Delta\epsilon_R$ is proportional to $Z^4 R^2$, and it is only the coefficient [$\frac{2}{5}$ in Eq. (11)] which depends on the nuclear charge distribution.

II. CORRECTIONS TO ENERGY LEVELS

It is now necessary to consider the detailed dependence of the results of Sec. I on the assumptions that have been made.

A. Meson Properties

1. Spin and Magnetic Moment

The μ^- meson has been assumed to have a spin of one half. For a point particle spins of one or larger, or a large anomalous magnetic moment are inconsistent with cosmic-ray burst data.¹¹⁻¹³ An anomalous magnetic moment of about eight times the normal Dirac moment would be necessary to increase the $2p_{3/2} - 1s_{3/2}$ transition energy by 0.5 Mev in lead. (Such an energy shift would lead to a radius of $1.3 \times 10^{-13} A^{1/3}$ cm from the experimental data.) The $2p_{3/2} - 2p_{1/2}$ level splitting would then be 1.44 Mev and should have been observed. (Experimentally a 0.2-Mev splitting is believed to have been observed, corresponding to the normal Dirac moment.)

Spin zero is inconsistent with the decays of the pi meson and the mu meson, if the neutral decay products are assumed to be neutrinos. Even if the meson spin is assumed to be zero, however, the energy levels obtained in Sec. I remain substantially unaltered. The reason for this is that the spin interaction is small, its largest effect being to produce a fine structure in various orbital angular momentum states. The absence of the $2p$ fine structure would decrease the maximum calculated $2p - 1s$ transition energy by a small amount.

¹⁰ H. Feshbach, Phys. Rev. **84**, 1206 (1951).

¹¹ R. F. Christy and S. Kusaka, Phys. Rev. **59**, 414 (1941).

¹² R. E. Lapp, Phys. Rev. **64**, 255 (1943); **69**, 312 (1946).

¹³ F. E. Driggers, Phys. Rev. **87**, 1080 (1952). Additional references are given here.

2. Mass

In the calculations reported in Table I the mass of the μ meson was taken to be $210m_e$, in agreement with the best measurements of this mass,^{14,15} as well as a good fit of all the Fitch and Rainwater data. For a point nucleus, the hydrogen-like meson energy levels (and transition energies) are directly proportional to the mass of the meson. For a uniformly charged nucleus, however, the potential inside the nucleus is harmonic [see Eq. (6)]. Thus the meson spends some time in a potential for which the transition energies are inversely proportional to the square root of the mass.¹⁶ The calculated $2p - 1s$ transition energies then are not directly proportional to the meson mass. In particular, for heavy nuclei ($A \sim 200$), where the probability of the meson being inside the nucleus is about one-half, the energy levels are quite insensitive to small variations in mass.

A perturbation procedure allows us to estimate the dependence of the energy levels on the meson mass as

$$\Delta\epsilon_{\mu k} = -(\epsilon_k - \bar{V}_k)\Delta\mu/\mu, \quad (12)$$

where ϵ_k is the energy for a meson of mass $210m_e$ in the state specified by the quantum number k , $\bar{V}_k = \langle \phi_k | V | \phi_k \rangle$, and $\Delta\mu$ is the change in meson mass. The term in parentheses in Eq. (12) represents the average kinetic energy of the meson in the state k .

For lead, with a nuclear radius $R = 1.4A^{1/3} \times 10^{-13}$ cm, a 5 percent increase in mass increases the $2p - 1s$ transition energy by about 0.2 percent, or 8.0 kev. This small change in energy means that the average kinetic energies in the $2p$ and $1s$ states are almost equal; exact equality would lead to no change in the transition energy for a small variation in mass. For a radius of $1.3A^{1/3} \times 10^{-13}$ cm, the increase in energy is approximately 14 kev. For a lighter nucleus, such as copper, on the other hand, a mass increase of only 0.7 percent increases the $2p - 1s$ transition energy by as much as 10 kev. In this case, then, to fit the experimental transition energy with a radius, $r_0 \approx 1.3 \times 10^{-13}$ cm, the meson mass required would be $215 - 216m_e$. A similar result is obtained for titanium, as shown in the accompanying paper by Fitch and Rainwater.

B. The Nuclear Ground State

In Part I the nuclear ground state proton charge distribution has been considered to be uniform and spherically symmetric.

1. Discreteness of Charge Distribution

In the above calculations the protons were replaced by a continuous distribution. This assumes implicitly

¹⁴ Lederman, Booth, Byfield, and Kessler, Phys. Rev. **83**, 685 (1951).

¹⁵ W. H. Barkas, University of California Radiation Laboratory Report UCRL-1285 (unpublished).

¹⁶ L. I. Schiff, *Quantum Mechanics* (McGraw-Hill Book Company, Inc., New York, 1949), p. 61.

that the meson wavelength is much larger than the average wavelength of the nucleons. For heavy atoms, however, the wavelength of a meson in the 1s state is of the order of magnitude of nuclear dimensions. An estimate of the effect of a discrete nuclear charge distribution can be obtained by calculating the interaction of a meson with a static nucleon lattice. The protons are arranged symmetrically on spherical shells, the number of protons on a shell and the spacing of the shells being so chosen that the radial variation of the potential produced gives no energy level shifts from the uniform distribution. The shifts in energy levels can then be calculated for a single shell by perturbation theory to second order. (The first order is zero.) These are negligible for light nuclei because of the large average distance of the meson from the nucleus. Even for a heavy nucleus such as lead, the deviation from the energy levels calculated in Part I is less than 0.1 percent (10 kev) for the 1s state.

2. Variations in the Ground-State Radial Charge Distribution

We consider next variations in the radial distribution of the nuclear charge. Since the observed maximum $2p-1s$ transition energy determines only one parameter, it is not possible to specify completely the nuclear charge distribution from this data. For comparison with other experiments it was convenient to use as this parameter the radius of the uniform charge distribution which fits the observations. This defines an "effective electromagnetic radius," which we saw to be $1.2A^{1/3} \times 10^{-13}$ cm.

For a given maximum charge density it is the uniform charge distribution which binds the 1s state meson most closely, and therefore gives the largest $2p_{3/2}-1s_{1/2}$ transition energy. This is so because the absolute value of the potential produced by a nonuniform charge distribution, with a fixed maximum density, is, from Gauss' law, always smaller than that of a uniform distribution with this maximum density. Thus any nuclear 'tail' or surface effect, without an increase in the maximum charge density, will decrease the $2p-1s$ transition energies.

Also the model with the proton density increased towards the edge of the nucleus as a result of Coulomb repulsion¹⁷ will decrease the electromagnetic potential inside the nucleus and thus decrease the binding of the 1s state.

The deviations from a uniform charge distribution considered above, all decrease the calculated transition energy. The latter can be increased only by increasing the proton charge density at the center of the nucleus. Some evidence for such a distribution has recently been obtained by Hofstadter,¹⁸ and analyzed by Schiff,¹⁹

¹⁷ E. Feenberg, Phys. Rev. **59**, 593 (1941).

¹⁸ Hofstadter, Fechter, and McIntyre, Phys. Rev. **91**, 439 (1953); also an article to be published.

¹⁹ L. I. Schiff, Phys. Rev. (to be published).

who finds a distribution compatible with $\rho(r) = Ze \exp(-r/a)/2a^3$. The potential V of such a distribution is [see Eq. (3)]

$$V_{\text{exp}} = -\frac{Ze^2}{r} \left\{ 1 - e^{-r/a} \left(1 + \frac{r}{2a} \right) \right\}. \quad (13)$$

At the origin this potential is $V_{\text{exp}}(r=0) = -Ze^2/2a$, whereas a uniform charge distribution gives $V_{\text{unif}}(r=0) = -3Ze^2/2R$. Therefore, unless $R/a > 3$, the exponential distribution will decrease the calculated $2p-1s$ transition energies.²⁰ V_{unif} and V_{exp} are compared in Fig. 2 for $R/a=3$ and $R/a=4$.

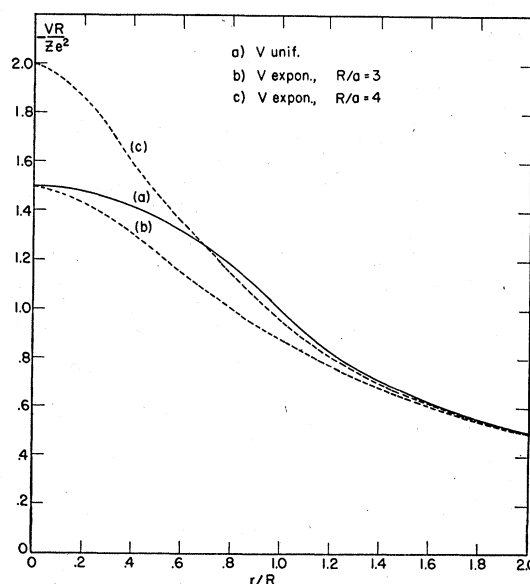


Fig. 2. Comparison of potentials produced by a uniform charge distribution of radius R and by an exponential charge distribution, $\rho \sim \exp(-r/a)$ for $R/a=3$ and 4.

3. Quadrupole Moment

There remains the possibility of asymmetries in the nuclear ground-state distribution. For nuclei with spins larger than one-half, such asymmetries generally give rise to quadrupole or higher moments. A nuclear quadrupole moment splits the $2p_{3/2}$ state into several levels. The magnitude of this level splitting has been calculated by Wheeler²¹ in an adjoining paper by assuming the quadrupole to arise from a nucleus distorted into the shape of a prolate or oblate ellipsoid. For a uniformly distributed charge inside such a nucleus, Wheeler finds the potential energy V to be

²⁰ A nonrelativistic perturbation calculation on the 1s-state energy level shows that for lead a must be of the order of 1.8×10^{-13} cm to correspond to a uniform charge radius of $1.2A^{1/3} \times 10^{-13}$ cm. R/a is then approximately 3.9.

²¹ J. A. Wheeler (following paper), Phys. Rev. **92**, 812 (1953).

(assuming the distortion from sphericity to be small):

$$V(r) = -\frac{Ze^2}{r} - \frac{1}{2}(3 \cos^2 \theta_{\mu I} - 1) \frac{Qe^2}{2r^3}, \quad r \geq R;$$

$$V(r) = -\frac{Ze^2}{R} \left(\frac{3}{2} - \frac{1}{2} \frac{r^2}{R^2} \right) - \frac{1}{2}(3 \cos^2 \theta_{\mu I} - 1) \frac{Qe^2 r^3}{2R^5}, \quad r \leq R.$$

The quadrupole moment Q is $Q = 2(c^2 - a^2)/5$, where c and a are the major and minor axes of the ellipsoid, respectively; these axes are related to the spherical radius R by $R^3 \approx a^2 c$. The interaction term which arises from the quadrupole moment decreases rapidly inside the nucleus, so that the splitting is smaller than on the basis of a point-charge interaction. A simple estimate of the quadrupole splitting of the $2p_{3/2}$ level is obtained by Wheeler on the assumption of a nonrelativistic (hydrogen-like) point nucleus wave function.

In general, the quadrupole splitting is much smaller than the fine structure splitting. Exceptions to this rule occur for intermediate and heavy nuclei, where large quadrupole moments cause the splitting of the $2p_{3/2}$ level to be of the same order of magnitude as that from spin orbit coupling. In principle, the splitting can be made use of to measure the quadrupole moment, or if the latter is known, to obtain further information about the nuclear charge distribution.

C. Nuclear Polarization

In calculating the energy levels of the mesonic atom we assumed the nucleus to be unaffected by the presence of the meson. The electromagnetic term H^e was therefore averaged over the nuclear ground state, to compute a potential in which the meson was taken to move. We now include induced nuclear effects (polarization) on the meson level structure by treating $H' = H^e - \langle \psi_0 | H^e | \psi_0 \rangle$ as a perturbation on the meson-nucleus Hamiltonian, $H^N + H_S$.

The first-order correction, $W^{(1)}$, to the total energy of the meson-nucleus system, $W = E + \epsilon$, is zero for any meson state. It is in the second-order correction, $W^{(2)}$, that nuclear polarization effects appear. For a meson in the state k ,

$$W^{(2)} = \sum_{\substack{N, m \\ N=0 \text{ with } m=k \\ \text{excluded}}} \frac{\langle \psi_0 \phi_k | H' | \psi_N \phi_m \rangle \langle \psi_N \phi_m | H' | \psi_0 \phi_k \rangle}{(E_0 + \epsilon_k - E_N - \epsilon_m)}, \quad (14)$$

where N and m refer to the entire set of quantum numbers for a given state and $N=0$ and $m=0$ are those for the ground state. $H' = H^e - V$ can be expanded in spherical harmonics,

$$H' = -e^2 \sum_{l=0}^{\infty} H'_l = -e^2 \sum_{l=0}^{\infty} \sum_{i=1}^Z f_l(r, R_i) P_l(\cos \theta_i), \quad (15)$$

where for $l=0$

$$\begin{aligned} f_0(r, R_i) &= 1/R_i + V/Ze^2, & r \leq R_i \\ &= 1/r + V/Ze^2, & R_i \leq r \leq R \\ &= 0, & R \leq r; \end{aligned}$$

and for $l>0$

$$\begin{aligned} f_l(r, R_i) &= r^l/R_i^{l+1}, & r \leq R_i \\ &= R_i^l/r^{l+1}, & r \geq R_i. \end{aligned}$$

Here θ_i is the angle between the meson and i th nucleon position vectors, and P_l are the Legendre polynomials.

The orthogonality of Legendre polynomials with different values of l allows us to rewrite Eq. (14) as

$$W^{(2)} = e^4 \sum_{l=0}^{\infty} W_l^{(2)},$$

where

$$W_l^{(2)} = \sum_{\substack{N, m \\ N=0 \text{ with } m=k \\ \text{excluded}}} \frac{\langle \psi_0 \phi_k | H'_l | \psi_N \phi_m \rangle \langle \psi_N \phi_m | H'_l | \psi_0 \phi_k \rangle}{(E_0 + \epsilon_k - E_N - \epsilon_m)} \quad (16)$$

for a k -state meson.

The polarization effects are largest for a $1s$ -state meson, for which they increase the binding energy. For a $2p$ state, where the average distance of the meson from the nucleus is much larger, the polarization effects are expected to be much smaller and may increase or decrease the binding energy.

$W_0^{(2)}$ can be interpreted as the system energy change resulting from a symmetric nuclear compression. In this term there are matrix elements which involve only changes in nuclear levels without any accompanying changes in meson levels (i.e. $N \neq 0$, $m = k$). In all higher-order terms (induced dipole, $l=1$; induced quadrupole, $l=2$; etc.) the nuclear transitions are always accompanied by meson transitions. In evaluating $W_l^{(2)}$ we perform closure over nuclear states; that is, the sum over nuclear states is performed by replacing the variable energy $E_0 - E_N$ by an average excitation energy.

For a $1s$ state meson, after the angular integrations have been performed, $W_l^{(2)}$ becomes

$$\begin{aligned} W_l^{(2)} &= \frac{Z}{2l+1} \sum_m \int d\mathbf{R}_i \int_0^\infty r^2 dr \int_0^\infty r'^2 dr' |\psi_0|^2 \\ &\quad \times R_0^*(r) R_{ml}(r) R_0(r') R_{ml}^*(r') f_l(R_i, r) \\ &\quad \times f_l(R_i, r') \frac{1}{\langle (E_0 - E_N) + \epsilon_0 - \epsilon_m \rangle}, \quad (17) \end{aligned}$$

where R_{ml} is the meson radial function, m is now only the principal quantum number, and l is the orbital angular momentum quantum number.

The evaluation of $W_l^{(2)}$ can be further simplified if we perform closure over the meson as well as nucleon

D. Specific Nuclear Interactions

Interactions between the μ^- meson and nucleus of non-electromagnetic origin so far have been neglected. One such reaction is the charge-exchange capture interaction $p + \mu^- \rightarrow n + \nu$. The strength of this interaction can be estimated from the coupling constant, which has been calculated to be of the order of that for β decay,^{6,22} (i.e., $\sim 3 \times 10^{-49}$ erg-cm³). This is equivalent to a potential of less than 100 ev for any nucleus, and has a negligible effect on the computed energy levels.

Another possible meson-nucleon interaction is one that does not contribute to the charge-exchange reaction but causes scattering. This might be a pair interaction term, $H = g \int \psi^* \phi^* \phi \psi d\tau$, which causes potential like scattering and meson pair creation and annihilation. If such an anomalous effective interaction potential is small (~ 1 Mev) and has a range $\sim r_0$, then it will be difficult to distinguish its scattering from the Coulomb scattering due to the nuclear charge. The reason for this is that such an anomalous potential has approximately the same effect as a small change in the nuclear charge distribution. If the form of the interaction is that indicated above, however, it might be observed by direct pair creation experiments.

Thus, one possible explanation of the small radius obtained by Fitch and Rainwater is to postulate an attractive anomalous meson-nucleus interaction. The depth of an effective potential of radius R would have to be approximately 1 Mev for lead, to increase the calculated mesonic x-ray radius to $1.3 \times 10^{-13} A^{\frac{1}{3}}$ cm. (The energy shift for any meson level is proportional to the depth of the potential and to the probability of finding the meson inside the nucleus; this probability is about one-half for the meson $1s$ state of lead.) There is presently little evidence for the anomalous interaction postulated above. The high-energy μ -meson anomalous scattering data of Amaldi²³ can be used to derive, in the Born approximation,²⁴ an equivalent potential. The data for lead and iron give an *upper* limit to the cross section per nucleon²³ of 4.5×10^{-29} cm². For lead and copper this gives a *maximum* potential of 0.8 and 0.4 Mev over the volume of the nuclei, and consequent $2p-1s$ transition energy shifts of about 0.4 and 0.03 Mev, respectively. However, the above limitations apply. Furthermore, Amaldi assumes spherically symmetric scattering to derive his maximum cross section. For lead, he observes only 13 large-angle scattering out of 73 000 total events, which suggests that a small proton contamination would be sufficient to materially alter the results. Thus, it is believed that such data cannot really be regarded as evidence for the existence of an anomalous scattering interaction.

²² J. M. Kennedy, Phys. Rev. **87**, 953 (1952).

²³ E. Amaldi and G. Fidicaro, Phys. Rev. **81**, 339 (1951).

²⁴ N. F. Mott and H. S. W. Massey, *The Theory of Atomic Collisions* (Oxford University Press, London, 1949), p. 120.

III. CONSISTENCY OF SMALL ELECTROMAGNETIC RADIUS

This section considers whether the effective electromagnetic radius determined by the μ^- -meson x-ray experiments is consistent with other measurements of the nuclear radius. These measurements can conveniently be separated into two groups. The first of these is sensitive to the nuclear charge distribution and consists chiefly of electron and proton scattering, isotope shifts of electron hyperfine structure, electron x-rays from heavy elements, and β -decay measurements. The second group depends upon a "nuclear force radius" and consists chiefly of neutron scattering, α -decay lifetime, and charged particle initiated nuclear reaction yield measurements.

A. Comparison with Experiments

1. Electromagnetic Radius

Measurements of both high-energy electron²⁵ and proton scattering²⁶ probe the nuclear proton distribution and have indicated an electromagnetic radius of the same order of magnitude as that determined by Fitch and Rainwater.

Isotope shifts of the electron hyperfine structure measure the change in proton charge distribution upon the addition of a neutron to the nucleus. The observed values of these shifts are approximately one-half those calculated on the basis of a constant nuclear density throughout a sphere of radius $R = 1.5 \times 10^{-13} A^{\frac{1}{3}}$ cm.²⁷ A possible explanation of this effect is an electromagnetic radius $R \approx 1.2 \times 10^{-13} A^{\frac{1}{3}}$ cm,²⁷ although other explanations have also been proposed.^{27,28}

Electron x-rays from heavy elements have been investigated by Schawlow and Townes²⁹ to deduce a nuclear charge distribution radius $R \approx 1.5 \times 10^{-13} A^{\frac{1}{3}}$ cm. It is possible, however, that changes in the nuclear charge distribution may make this experiment agree with the μ -meson results.

β -decay data for mirror nuclei have been used to obtain an electromagnetic radius $R = 1.4 - 1.5 \times 10^{-13} A^{\frac{1}{3}}$ cm.³⁰ It will be shown in part B, however, that corrections to the usual calculations tend to reduce this estimate considerably.

2. Nuclear Force Radius

Fast neutron scattering experiments³¹ have been analyzed on an optical model to give a nuclear radius

²⁵ Lyman, Hanson, and Scott, Phys. Rev. **84**, 626 (1951).

²⁶ Richardson, Ball, Leith, and Moyer, Phys. Rev. **83**, 859 (1951); K. M. Gatha and R. D. Riddell, Jr., Phys. Rev. **86**, 1035 (1952).

²⁷ M. F. Crawford and A. L. Schawlow, Phys. Rev. **76**, 1311 (1949).

²⁸ Willets, Hill, and Ford, Phys. Rev. **91**, 1488 (1953).

²⁹ A. L. Schawlow and C. H. Townes, Science **115**, 284 (1952).

³⁰ J. M. Blatt and V. F. Weisskopf (see reference 9, Chap. VII, especially Sec. 2).

³¹ Cook, Macmillan, Peterson, and Sewell, Phys. Rev. **75**, 7 (1949).

$R=1.3-1.4 \times 10^{-13} A^{\frac{1}{2}}$ cm.³² It is essential to note that these measurements determine a "nuclear force radius" rather than a proton distribution radius. The sensitivity of the calculated radius to variations in the distribution of nuclear matter has not been investigated in detail.

Both α -decay lifetimes and the yield of charged particle initiated nuclear reactions indicate nuclear radii⁹ $R=1.35-1.6 \times 10^{-13} A^{\frac{1}{2}}$ cm. These experiments measure chiefly the transparency of the Coulomb barrier which is superimposed on the nuclear force potential. They thus depend on the radius at which the repulsive Coulomb force becomes larger than the nuclear force but are uncertain because of the unknown size of the escaping or entering particles. It has been shown by Wheeler³³ that, on the basis of a strong coupling nuclear collective model, the α -decay radius is expected to be larger than that of the charge distribution because of the nuclear deformation.

B. Mirror Nuclei

The maximum β -decay energies for mirror nuclei, which specifically depend on the proton charge distribution, seem to require an electromagnetic radius $R=1.4-1.5 \times 10^{-13} A^{\frac{1}{2}}$ cm.

Since the mirror nuclei measurements are for $Z \leq 21$, and the other electromagnetic experiments are more accurate for heavier elements, it might be argued that no real discrepancy exists, and that the electromagnetic radius increases for light elements. However, the following considerations indicate that such an assumption need not be made, and that a radius $R \approx 1.2 \times 10^{-13} A^{\frac{1}{2}}$ cm can be made consistent with mirror nuclei experiments.

The difference in Coulomb energy of parent and daughter nuclei is calculated usually by assuming that a nucleon initially distributed uniformly over the nuclear sphere makes the transition. The Coulomb energy change, ΔE_c , for the reaction $A^{Z+1} \rightleftharpoons A^Z$ is then

$$\Delta E_c = (6/5)(Ze^2/R). \quad (20)$$

In this, the nucleus is assumed to have the same initial and final radius. A simple calculation that allows for the proton sphere to change in the β -decay transition, due to the difference in Coulomb energy between the mirror nuclei, does not alter the above materially.

It will be shown below that it is impossible to make mirror nuclei and mesonic atom experiments consistent by merely changing the charge distribution, if it assumed that all protons have the same distribution and that the nuclear charge density is positive definite. (If a negative meson cloud existed which made the charge distribution vary in sign, then the two experiments could be made consistent with a charge distribution variation.) However, it will then be demonstrated that relaxation of the first condition above (all protons

having the same charge distribution), together with angular momentum considerations, as well as the antisymmetrization of the nuclear-proton ground state wavefunction can make the two experiments agree.

For an arbitrary charge distribution, it is the difference of the electrostatic energy

$$\int \rho_1(\mathbf{r})U(\mathbf{r})d\mathbf{r} \quad (21)$$

between the nuclei Z and $Z \pm 1$ that is determined by β -decay experiments. Here $U(\mathbf{r})$ is the potential determined by the charge distribution $\rho = Z\rho_1$ and is related to the previous V by $V = -eU$. As stated previously, it is the integral

$$\int (U - Ze/r)d\mathbf{r} \quad (22)$$

that is determined by both high-energy electron scattering (less than ~ 40 Mev) and by the μ^- -meson experiments for low Z . For a uniform charge distribution, where a radius $R \approx 1.2 \times 10^{-13} A^{\frac{1}{2}}$ cm is needed to fit the mesonic x-ray data, the integral (21) is too large to fit the observed Coulomb energy change in β decay.

To determine if a charge distribution exists which decreases this discrepancy, the integral (21) was minimized, keeping Eq. (22) and the total charge constant. If dV/dr is continuous, a partial integration of (21) gives

$$(1/Z) \int (\nabla U)^2 d\mathbf{r}.$$

The usual variation calculation then leads to a stationary value for

$$\nabla^2 U = \text{constant.} \dagger$$

This corresponds to a uniform charge distribution. The resultant potential has been shown explicitly to give a smaller value for (21), under the auxiliary conditions, than a shell of charge or a charge distribution $\rho = A - Br$.

Thus the integral (21) is a minimum for a uniform charge distribution. This means that, under the assumptions made (including ρ positive definite) any non-uniform charge distribution increases the discrepancy between the meson-transition and β -decay results.

However, it is possible to construct nuclear models which, with the inclusion of (a) Coulomb exchange

† Note added in proof.—A similar result was obtained independently by Bitter and Feshbach (private communication). The restriction to positive definite ρ was not included explicitly in either proof so that the cutoff of ρ at $r=R$ had to be introduced ad-hoc. The restriction to positive ρ can be included explicitly by varying $s = (\rho)^{\frac{1}{2}}$, i.e., $s = s_0 + \delta s$. The variational calculation then gives

$$\int_0^\infty s_0 \delta s r^2 (V_0 + \gamma + \lambda r^2) dr = 0.$$

Thus $V_0 + \gamma + \lambda r^2 = 0$ only if s_0 (or ρ_0) $\neq 0$. It can then easily be shown that

$$\begin{matrix} \rho_0 = \text{constant} & \text{for } r < R \\ \rho_0 = 0 & \text{for } r > R \end{matrix}$$

is the minimum value.

³² Fernbach, Serber, and Taylor, Phys. Rev. 75, 1352 (1949).

³³ D. L. Hill and J. A. Wheeler, Phys. Rev. 89, 1102 (1953).

energy and (b) angular momentum effects, reduce the above estimate of mirror nuclei radii. The difference in Coulomb energies for these nuclei is calculated below for a statistical model and a shell model.

In the Hartree approximation the Coulomb energy of a nucleus with Z protons is, after summing over spin coordinates,

$$E_c = \frac{1}{2} \sum_{i=1}^Z \sum_{j=1}^Z \int |\psi_i(\mathbf{R}_1)|^2 |\psi_j(\mathbf{R}_2)|^2 \frac{e^2}{R_{12}} d\mathbf{R}_1 d\mathbf{R}_2 - \frac{1}{4} \sum_{i=1}^Z \sum_{j=1}^Z \int \psi_i^*(\mathbf{R}_1) \psi_j(\mathbf{R}_1) \psi_i(\mathbf{R}_2) \times \psi_j^*(\mathbf{R}_2) \frac{e^2}{R_{12}} d\mathbf{R}_1 d\mathbf{R}_2, \quad (23)$$

where ψ_i are the equivalent central potential proton wave functions. The first term in Eq. (23) is the direct Coulomb energy, while the second term is a Coulomb exchange energy arising from the antisymmetrization of the ground-state proton wavefunctions.³⁴

Equation (23) is evaluated first for a nuclear statistical model. This yields a uniform charge distribution for the protons, so that the direct term gives the usual nuclear electrostatic energy. We obtain (if $A = 2Z$)

$$E_c(Z) \approx \frac{3}{5} \frac{Z(Z-1)e^2}{R} - 0.46 \frac{Z^{4/3}e^2}{R}. \quad (24)$$

This result has been derived previously by Bethe and Bacher,³⁵ and Weizsacker.³⁶ The exchange term is significant for small values of Z , where mirror nuclei measurements are made. If the effective nuclear radius found from Eq. (24) is $R = r_0 A^{1/3}$, then

$$r_0 = r_0' (1 - 0.51Z^{-2/3}),$$

where r_0' is the radius calculated from the direct term alone. r_0 is smaller than r_0' and varies slowly with Z ; for $Z = 15$, r_0 is about 9 percent smaller than r_0' . Thus, the inclusion of the exchange term alone, reduces the radius of the uniform charge distribution deduced from β decay from an average of $1.45 \times 10^{-13} A^{1/3}$ cm to about $1.3 \times 10^{-13} A^{1/3}$ cm.

Equation (23) was also evaluated for a nuclear shell structure. For simplicity, an infinite square well potential was chosen. Here the protons are not distributed uniformly throughout the nucleus, and the nucleon which undergoes β decay will have a different charge distribution than the average of the other protons. The proton distribution therefore need not remain unchanged in the transition. In fact, for a nuclear shell model, as assumed here, the β -decay nucleon is usually

³⁴ E. Feenberg and G. Goertzel, Phys. Rev. **70**, 597 (1946) (additional references are listed here).

³⁵ H. A. Bethe and R. F. Bacher, Revs. Modern Phys. **8**, 162 (1936).

³⁶ C. F. von Weizsacker, Z. Physik **96**, 431 (1935).

in a higher angular momentum state than the other protons. The change in Coulomb energy for such a transition is less than is expected for a uniformly distributed particle, because the radial distribution of higher angular momentum states is weighted more heavily towards the periphery of the nuclear sphere, where the potential of the nuclear charge distribution is smallest in magnitude. An extreme of this model was considered by Bethe,³⁷ who assumed the extra nucleon to be free.

The radius of the square well R_w is chosen so that the resulting proton charge distribution produces an electric potential which satisfies the meson experiment; that is, the integral (22) gives the same value for this potential as when evaluated for a uniform charge distribution of radius $R = 1.2 \times 10^{-13} A^{1/3}$ cm. The well parameter is assumed to remain constant in the reaction, since this parameter is determined by the nuclear forces which are assumed to be charge symmetric. The Coulomb

TABLE IV. Shell model calculation for mirror nuclei radii. $R = r_0 A^{1/3} \times 10^{-13}$ cm. $R_w = r_{0w} A^{1/3} \times 10^{-13}$ cm is the radius of the infinite well such that the charge distribution produced by this well makes the integral $\int_0^\infty (V - V_p) r^2 dr$ fit the μ^- -meson experiment with an effective meson radius $R_M = r_{0M} A^{1/3} \times 10^{-13}$ cm; $r_{0(D)}$ and $r_{0(D+E)}$ are those r_0 which, when substituted in Eq. (20), give the ΔE_c calculated on the infinite well model for the removal of a single proton above the closed shells. $r_{0(D)}$ includes only the direct term of Eq. (23) while $r_{0(D+E)}$ includes both direct and exchange terms. r_{0u} is the usual mirror nucleus radius adjusted so that Eq. (20) gives the observed maximum β -decay energy.

Z	r_{0w}	Effective meson radius r_{0M}	$r_{0(D)}$	Calculated effective mirror nucleus radius $r_{0(D+E)}$	Observed effective mirror nucleus radius r_{0u}
$3 \rightleftharpoons 2$	1.78	1.2	1.29	1.53	...
$9 \rightleftharpoons 8$	1.69	1.2	1.36	1.53	1.39
$19 \rightleftharpoons 18$	1.55	1.2	1.20	1.25	1.47
$21 \rightleftharpoons 20$	1.59	1.2	1.36	1.54	1.50
$35 \rightleftharpoons 34$	1.38	1.2

energy change due to the addition of a proton to the above charge distribution is then calculated, and consists of two terms. The first, the direct term, will differ from that in Eq. (20) for the reasons discussed above, while the second term is the exchange energy. This was evaluated as in Condon and Shortley.³⁸ Calculations were performed for closed shell nuclei because a coupling scheme does not have to be specified here. Numerical results are presented in Table IV.

For a nonclosed shell nucleus the same qualitative result is obtained, as shown by the following simple considerations. The Coulomb interaction of the single proton, which is involved in the transition, with the closed shells is of the same order of magnitude as calculated above for the single nucleon above a closed shell. The Coulomb interaction of this proton with other protons in the same shell is more difficult to estimate,

³⁷ H. A. Bethe, Phys. Rev. **54**, 436 (1938).

³⁸ E. U. Condon and G. H. Shortley, *The Theory of Atomic Spectra* (Macmillan Company, New York, 1935), Chap. VI.

since this depends upon specific coupling assumptions. If we assume no coupling between single particle wave functions, then the exchange interaction becomes very large because the radial wave functions are identical, and this reduces the Coulomb energy considerably.

From Table IV and the qualitative discussion above, we see that, except for the 2s state, the inclusion of the Coulomb exchange term and angular momentum considerations are sufficient to explain the mirror nuclei data with a radius as small as that required by Fitch and Rainwater. This conclusion depends upon the nuclear model chosen; it is possible, of course, to construct models which minimize the above effects.

CONCLUSION

Experimental evidence obtained from the study of mesonic x-rays indicates a larger nuclear proton density than has heretofore been accepted. For a constant nuclear charge density, the measured $2p-1s$ transition energies can be understood in terms of a nuclear electromagnetic radius of about $R=1.2\times 10^{-13}A^{\frac{1}{3}}$ cm.

With the usual nuclear radius ($1.35-1.5\times 10^{-13}A^{\frac{1}{3}}$ cm) the experimental transition energies cannot be explained by nuclear polarization and other effects discussed, except for an anomalous meson-nucleus interaction; however, there is presently little evidence for such an interaction.

Comparison of the present results with previous electromagnetic radius measurements show general agreement, except for electron x-ray measurements. This agreement holds for mirror nuclei experiments, when calculations take into account Coulomb exchange energies and angular momentum considerations.

We wish to thank above all Professor R. Serber for many valuable discussions and Professor J. Rainwater and Dr. V. L. Fitch for communicating and discussing their results prior to publication. We also wish to thank Professor C. H. Townes and Dr. M. A. Ruderman for helpful discussion and Professor J. A. Wheeler for making available his calculations prior to publication.†

† *Note added in proof.*—The authors are grateful to Professors L. L. Foldy and N. Kroll for pointing out to them that electrodynamic effects are not negligible. In particular, to lowest order in Z , the dominant term is caused by the polarization of the vacuum due to electron pairs. This gives a contribution [see for example R. Karplus and N. Kroll, Phys. Rev. 77, 540 (1950)] in particular $D_F^{(2)}$ which increases the potential V by

$$\frac{2}{3\pi}\alpha V(r)[\ln(1/m_e r) - 5/6].$$

There is presently no method for evaluating higher order Z corrections. The above increase in potential of somewhat less than

APPENDIX A

The term in $W_0^{(2)}$ which involves no meson transitions, $W_{00}^{(2)}$, is

$$W_{00}^{(2)} = \frac{1}{\langle E_0 - E_N \rangle} \langle \phi_k(r) \phi_k(r') \rangle \times |\langle \psi_0 | H_0'(r) H_0'(r') | \psi_0 \rangle| \phi_k(r) \phi_k(r'), \quad (A1)$$

where closure over nucleon states has already been performed. The substitution

$$H_0' = \sum_{i=1}^{Z'} f_0(r, R_i) P_0(\cos\theta_i),$$

according to Eq. (15), gives

$$W_{00}^{(2)} = \frac{1}{\langle E_0 - E_N \rangle} \sum_{i=1}^Z \sum_{j=1}^Z \int d\mathbf{R}_1 \cdots d\mathbf{R}_i \cdots d\mathbf{R}_j \cdots d\mathbf{R}_Z \times \int_0^\infty r'^2 dr' \int_0^\infty r^2 dr |\psi_0|^2 |R_{00}(r')|^2 |R_{00}(r)|^2 \times \left\{ T(R_i r) T(R_j r') + \frac{V(r)V(r')}{Z^2 e^4} \right\}, \quad (A2)$$

where

$$T(R_i r) = 1/R_i \text{ for } r < R_i, = 1/r \text{ for } R_i < r.$$

In Eq. (A2) there are $Z(Z-1)$ terms with $i \neq j$, which are zero because the two expressions inside the brace cancel. For the remaining Z terms we obtain (for a uniform nuclear density to R)

$$W_{00}^{(2)} = \frac{Z}{\langle E_0 - E_N \rangle} \left[\frac{3}{R^3} \int_0^R R_i^2 dR_i \int_0^R |R_{00}(r)|^2 r^2 dr \times \int_0^R |R_{00}(r')|^2 r'^2 dr' T(R_i r) T(R_i r') - \left\{ \frac{3}{R^3} \int_0^R R_i^2 dR_i \int_0^R |R_{00}(r)|^2 T(R_i r) r^2 dr \right\}^2 \right]. \quad (A3)$$

This equation has been integrated numerically to give the result reported in Table III.

$\frac{1}{2}$ percent for lead increases the $2p-1s$ transition energy by approximately 1 percent, which in turn leads to a 1 percent larger radius, R , for this element.